INTERNATIONAL JOURNAL OF ENERGY RESEARCH
Int. J. Energy Res. 2010; **34**:284–292
Published online 9 November 2009 in Wiley InterScience
(www.interscience.wiley.com). DOI: 10.1002/er.1634

Tomographic diagnostics of current distributions in a fuel cell stack

J. A. Hirschfeld[1,*,†], H. Lustfeld[2], M. Reißel[3] and B. Steffen[4]

[1]*Forschungszentrum Jülich, IAS-1, 52425 Jülich, Germany*
[2]*Forschungszentrum Jülich, IFF-1, 52425 Jülich, Germany*
[3]*Fachhochschule Aachen, Abteilung Jülich, 52428 Jülich, Germany*
[4]*Forschungszentrum Jülich, JSC, 52425 Jülich, Germany*

SUMMARY

A novel tomographic scheme for analysing the state of any single membrane electrode assembly (MEA) in a stack is suggested. Plates of very high conductivity placed between every fuel cell and slitted in an appropriate manner cause surface currents at well-defined locations of the stack. We show that knowing these surface currents, information about anomalies of the currents in a MEA can be obtained using the methods of tomography. The results are mathematically not unique. However, when assuming plausible defect structures, one can exclude improbable deficiencies by applying a special form of simulated annealing. We present numerical calculations of typical examples demonstrating that the essential defects of the MEA in any single cell of the stack can be detected and their extent can be determined.

KEY WORDS: defect detection; degradation; stack; fuel cell; current density distribution; tomography; MEA; DMFC; PEMFC

1. INTRODUCTION

It is not a trivial engineering task to keep a single fuel cell in a stable state [1], even if the power requirements remain constant. Its state and efficiency depend on temperature, on the state of the electrolyte and furthermore on fuel as well as exhaust gas conditions [2–6]. All this favours irregularities in the local electric current density produced by the membrane electrode assembly (MEA). Therefore the local current density can differ by a factor up to 1.5–3 in a single MEA (Wippermann, private communication) [7–9]. These problems accumulate in the stack, because fluctuations of the electric current density, still acceptable in a single cell, may accumulate due to the fact that electric currents of adjacent single cells can influence each other [10]. Therefore, the following requirements are important:

(a) To prevent current density fluctuations in one cell from spreading to neighbouring cells.
(b) To have a good diagnostics available by which irregularities of the electric currents in one cell can be detected opening the possibility of changing parameters and thus reducing those irregularities.

For a single cell some diagnostic methods to gain knowledge about the current density distribution

*Correspondence to: J. A. Hirschfeld, Forschungszentrum Jülich, IAS-1, 52425 Jülich, Germany.
†E-mail: j.hirschfeld@fz-juelich.de

Received 24 April 2009
Revised 7 September 2009
Accepted 17 September 2009

are known. Three methods have been presented by Stumper *et al*. [11], the partial MEA approach, the sub-cell method and the current distribution mapping. The last method is the most advanced one of these three, because it provides a high-resolution current density map by measuring the current directly at many locations of the cell. Although this method is highly advanced, it can only be applied to a single fuel cell and is not eligible to be applied to a fuel cell in a commercial product. Diagnostic methods that can be applied to a fuel cell stack are the electrochemical impedance spectroscopy [12,13] and the current interruption method [14]. By these methods one can gain knowledge about different kinds of defects in a particular fuel cell of a stack. However, they provide only integrated information for a whole cell. A further possibility consists of measuring the magnetic field and obtaining information about inner currents by applying magnetotomography [15]. At first sight, this method looks very promising, but suffers from the difficulty that the fields to be measured are small (of a fraction of the magnetic field of the earth). In fact hitherto the method has only been discussed for single cell problems [16].

In a previous paper [17], from now on denoted by I, we have developed a scheme [18] that fulfils both requirements. The idea is simple. Highly conducting thin plates (e.g. made of aluminium) positioned between the cells will enforce a smoothing of the normal (parallel to the axis of the stack) currents in the MEAs of the cells. Now slits appropriately placed in those plates will guide the transverse currents to the surface of the stack, where they can be detected, cf Figure 1. The principle demonstrated in Figure 2 for a plate with two slits can easily be generalized: plates with N slits virtually divide the MEA into $(N+1)\times(N+1)$ segments. From this the error of positioning a local disturbance can easily be determined. In fact, it is impossible to state where in a segment the local disturbance occurs.

When investigating how failures of normal currents in these virtual segments are related to the transverse surface currents one recognizes a clear advantage of the method: $2N$ measurements yield information of about $(N+1)\times(N+1)$ segments of the MEA. In fact, a degradation in just one segment of the MEA can quite easily be detected from surface current measurements. On the other hand, this advantage leads of course to uncertainties since one needs information about a number of segments much larger than the

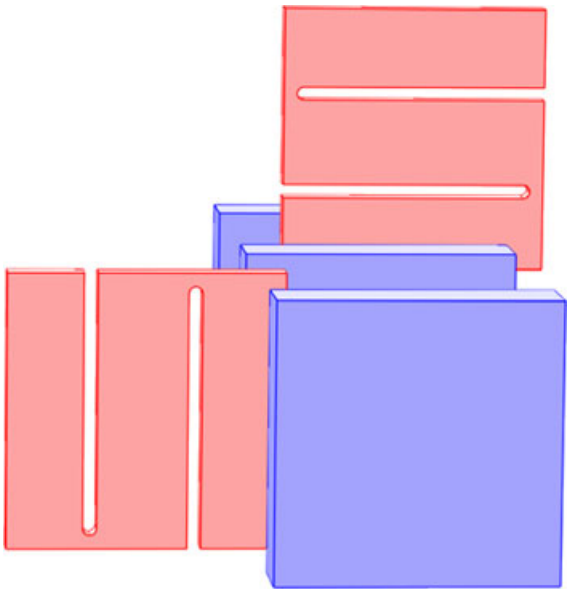

Figure 1. Exploded view of the diagnostic scheme. The full (blue) plates represent individual fuel cells, while the slitted (red) ones represent the metal plates.

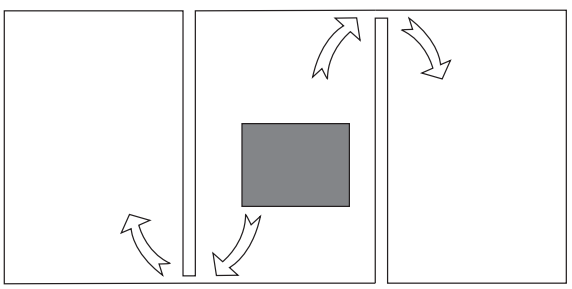

Figure 2. The principle of enforcing transverse currents to the surface of the stack can be understood from this figure: behind the plate with high conductivity a MEA is assumed that does not work in the grey shaded area. Therefore, the current coming from the previous MEA must be redirected away from this area. Due to the slits the major part of the current must go through the bridges connecting the inner part of the plate with the outer ones.

DOI: 10.1002/er

number of points where measurements are taken. Therefore, there is a clear lack of information. To give an example, a change of current in each segment by the same amount does not lead to surface currents at all and therefore cannot be detected by this method. But this is only one example of the many possible ambiguities. Indeed, in analogy to many tomographical problems, we have the following, not unusual situation: any change of the normal current in one or more segments leads to a unique change of the currents appearing at the surface of the stack. (This means in tomographic language the forward problem is unique.) However, the inverse is not true: from the surface currents we do not gain complete information to determine the currents in the virtual segments of the MEA in a unique way (in other words, the inverse problem is not unique).

As in analogous tomographic problems, the merit of the method depends on how important the missing information is. We show in this paper that the information lost is not essential for detecting failures. The reason is: typical failures in an MEA, those beginning at certain positions and their (perhaps not small) neighbourhoods, can be detected by our method.

In its present form the scheme is most easily applied to stacks with graphite flow field plates and operating temperatures below 200°C. As mentioned before requirement (a) is fulfilled by the addition of the highly conducting plates to the stack leading to lateral currents, which smooth irregularities of the electric current distribution. The appearance of lateral currents in fuel cells and fuel cell stacks is well known and has been investigated over the last years by several researchers [19–22]. However, in I it has been shown that these currents can also be used for diagnostic purposes by applying the above-described scheme, thus fulfilling the prerequisites for requirement (b). The reason has been given above: due to the slits, these currents are forced to the surface, where they can be detected.

The essential question is of course how big this effect is. By applying extensive computations for realistic materials we could show that the currents at the surface are detectable with sufficient precision by cheap measuring devices, at least for the case that the flow fields consist of graphite (e.g. Eisenhuth Sigracet PPG86). That the degree of failure of an area in the MEA could be determined from the transverse surface currents in those plates had been shown in I for simple cases.

In the present paper we deal with the general case of a failure in the MEA. In Section 2 we present computations of the surface currents in the highly conducting plates for a given normal current distribution in a cell of the stack. In Section 3 we discuss how to get the necessary information about the current distribution on a MEA in spite of the fact that the information obtained from measurements of the surface currents is intrinsically incomplete. We can show that very plausible assumptions about the kind of the irregular current distributions result in mathematical constraints, restricting the possible solutions to an extent, where unique conclusions are possible. As in any tomographic problem restricting solutions by constraints leads to a relatively sophisticated mathematical apparatus (cost functions with Lagrange parameters, search for absolute minima by applying simulated annealing, etc.). However, the representation of the method does not require all the involved mathematics, therefore this section stresses the essential points. For the mathematically interested reader we give a more detailed presentation of the mathematical apparatus in the appendix. In Section 4 we present typical current distribution anomalies in the MEA of a stack that can be successfully reconstructed from measurements of the slit currents, which are surface currents at the location of the slits (cf. Figure 2). The conclusion ends the paper.

2. CURRENT DISTRIBUTION IN A MEA AND SURFACE CURRENTS

In this section we describe the computation of the surface currents for a given current distribution in a defective MEA. The computations can be done by considering the arrangement described in Figure 3. Only the normal component of the current density in the defective MEA is of importance, which means that this component can be used as Neumann boundary condition for the current distribution in the metallic plate and

DOI: 10.1002/er

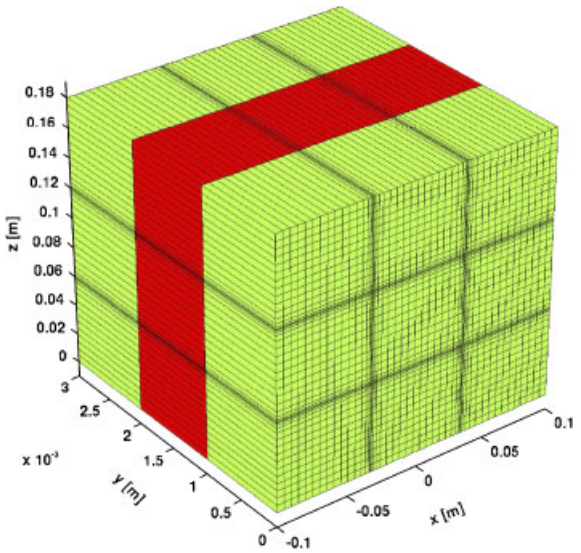

Figure 3. In this figure the arrangement for calculating the slit currents is shown. The boundary defining the normal current distribution of the defective MEA is in the foreground, behind it the flow field for this MEA (note the different scale in y-direction). The thin metallic plate with high conductivity follows, after that the flow field in front of the next MEA. The numerical grid in use for the computations is also shown. The positions of the slits in the central plate can be found by comparing Figure 2 with the local refinement of the grid.

the two flow fields. As in a very good approximation the normal current is uniform after passing the metallic plate, the second MEA need not be considered directly. Rather we can replace it by the Neumann boundary condition, which in that case is just the constant I_0/F, where I_0 is the total stack current and F is the area of the MEA. In spite of these simplifications, a three-dimensional partial differential equation has to be solved. The solution depends of course linearly on the boundary conditions representing the normal current of the defective MEA. This means: if the metallic plate contains N slits dividing the defective MEA into $N_{\mathrm{seg}} = (N+1) \times (N+1)$ virtual segments, then we solve the differential equation for N_{seg} different boundary conditions. (One possibility is setting the normal current to zero except in segment i, where the current is set to 1.) In this way, a matrix relation is obtained between the normal MEA currents across the segments $\mathbf{i}_{\mathrm{seg}}$—which in that resolution build N_{seg} dimensional vectors—and the N dimensional vector describing the surface currents going through the N bridges connecting the different parts of a metallic plate. We call these currents *slit currents* i_{S}. Their number is equal to the number of slits. For the calculations we used the following quantities:

- $\sigma_{\mathrm{graphite}} = 5.6 \times 10^3\,\mathrm{S\,m^{-1}}$ (Eisenhuth Sigracet PPG86 flow field plates)
- $\sigma_{\mathrm{Al}} = 4 \times 10^7\,\mathrm{S\,m^{-1}}$ (slitted aluminium plates)
- Fuel cell cross section: 200 mm × 180 mm, 1 mm plate thickness
- 1 mm slit width and 1 mm bridge width
- $I_0 = 60\,\mathrm{A}$ (total stack current)

The same procedure as before can be applied when calculating the slit currents in the metallic plate of high conductivity ahead of the defective MEA. Together with the other matrix relation one gets a linear relation between normal currents in the MEA and the $2N$ slit currents:

$$\mathscr{A} \cdot \mathbf{i}_{\mathrm{seg}} = \mathbf{i}_{\mathrm{S}}, \quad \text{for const. } \mathbf{I}_0 \tag{1}$$

(When writing down this equation it is assumed that the normal current density is the same on both sides of a MEA. This approximation is a very plausible one having been discussed as the *thin MEA approximation* [23,24].)

The computation of the matrix $\mathscr{A}$ requires some CPU time. However, if all the single cells of the stack are identical, it has to be computed only once for the inner cells and once for the first and last cell, where the conditions are different.

Equation (1) describes the tomographic problem and since $\mathscr{A}$ is a nonquadratic matrix it is quite clear that this equation is not sufficient to determine $\mathbf{i}_{\mathrm{seg}}$ in a unique way. Therefore, we have to look for constraints selecting the physically interesting solutions. This will be done in the next section.

Equation (1) is applicable as long as just one cell in the stack fails. Of course that need not be the case. However, if two cells are not adjacent, their irregularities do not interfere because the metallic plates will prevent any interaction between them and they can be treated independently [17,24]. Furthermore, if the damage of cells is rather accidental, it is improbable that two malfunctioning cells are

DOI: 10.1002/er

neighbours and we do not discuss this case in the present paper. However, it is quite clear that this situation can be treated in a quite analogous manner.

3. TOMOGRAPHIC CONSTRAINTS

As previously mentioned, the information about the segment currents $\mathbf{i}_{\text{seg}}$ is incomplete. To select physically relevant solutions we introduce constraints. Here we are interested in possible degradation of a single fuel cell and in this case we have to select solutions with increasing internal resistance. To formulate this as a constraint for the currents, we replace for the moment the condition of constant total current I_0 by the condition of constant voltage drop U_0 and denote the corresponding currents by $i_{\text{seg}'}$. Starting from the ideal situation for the segment currents we obtain as equivalent condition

$$i_{\text{seg}',n} \leqslant i_0 \quad \text{with } i_0 = \frac{I_0}{N_{\text{seg}}} \quad \text{and} \quad U_0 \text{ const.} \tag{2}$$

The slit currents $\mathbf{i}_{\text{S}}$ are given for constant I_0. The equivalent values $\mathbf{i}_{\text{S}'}$ for constant voltage drop U_0 are given by

$$\mathbf{i}_{\text{S}'} = \mathbf{i}_{\text{S}} \cdot \frac{1}{I_0} \sum_{n=1}^{N_{\text{seg}}} i_{\text{seg}',n} \tag{3}$$

With this we obtain an equation for the currents through the segments, equivalent to Equation (1) but with simply formulated constraints:

$$\mathscr{A} \cdot \mathbf{i}_{\text{seg}'} - \mathbf{i}_{\text{S}} \cdot \frac{1}{I_0} \sum_{n=1}^{N_{\text{seg}}} i_{\text{seg}',n} = \mathbf{0} \tag{4}$$

At the end we can obtain the segment currents i_{seg} for given I_0 by using Equation (3)

$$\mathbf{i}_{\text{seg},n} = \mathbf{i}_{\text{seg}',n} \cdot I_0 \cdot \left(\sum_{n=1}^{N_{\text{seg}}} i_{\text{seg}',n} \right)^{-1} \tag{5}$$

We mention that the increased voltage drop U_{new} is given by

$$U_{\text{new}} = U_0 \cdot I_0 \cdot \left(\sum_{n=1}^{N_{\text{seg}}} i_{\text{seg}',n} \right)^{-1} \tag{6}$$

$I_0(U_{\text{new}} - U_0)$ is the reduced power of the fuel cell in question and gives an information about the state of that cell. It can be used to look for segment currents $i_{\text{seg},n}$ compatible with Equation (4) but with the least reduction of efficiency.

As a further constraint we choose solutions favouring localization. The assumption here is that a deficiency starts more or less from a certain position and then is spreading out from there [10]. Such solutions have the property that $i_{\text{seg},i} - i_0 \approx 0$ for most i except for a few numbers. A function favouring these solutions is

$$f(i_{\text{seg}}) = \sum_{1}^{N_{\text{seg}}} \ln((i_{\text{seg},n} - i_0)^2 + \varepsilon), \quad \varepsilon > 0 \tag{7}$$

because f is the smaller the more localized the current decrease is. Furthermore the smaller ε, the steeper f becomes. ε is a dimensionless parameter defining how strong the localization should be. It turns out that the solutions depend over a wide range only weakly on it. Our approach is similar to the minimum entropy inversion [25].

As will be shown in the next chapter, these constraints lead already to a unique or nearly unique solution in most cases. However, we would like to point out that depending on the situation, other constraints may be preferred and are possible. The results in the next section demonstrate that with only a few constraints the picture of the current distribution in a certain MEA can become unique.

4. RESULTS

In this section we present three typical examples in which numerically generated patterns of MEA-failures are reconstructed by the procedures developed in Sections 2 and 3. The results of the reconstruction are then compared with the original pattern. We also look at the results as functions of the parameter ε because the dependence on ε gives a hint how strongly the results will depend on the special form of functions favouring localization.

We begin with a simple and complete failure in a single segment of the MEA for a 3×3 resolution. The numbering is that of Figure 4. As can be seen from Figure 5 the agreement between original and reconstructed pattern is excellent indeed and does not change even if ε increases by two orders of magnitude.

DOI: 10.1002/er

Similar are the trends in the more complex examples 2 and 3, cf. Figures 6 and 7. Example 2 is remarkable in so far, as the failure, though not complete, extends over a whole stripe. Such a failure may occur, if there is a disturbance in the fuel supply. The reconstruction works well even in this case.

If the damage of a cell is really extended, then the solution obtained from reconstruction can become two-fold degenerate [24], one agrees completely with the original disturbance the other one is more or less different. However, the power loss is correctly obtained. It is also remarkable that the degenerated solutions do not change even if ε changes by two orders of magnitude [24]. We think that this degeneracy could be removed as well, but here we suffer from a lack of information about further typical characteristics of MEA damages.

Anyway, the main result of all the examples considered so far is twofold: If a not too extended damage occurs, the surface currents yield sufficient information for identifying the kind and its relevance. Only if a damage is extended *and* occurs suddenly the information may not be unique but at least the actual power loss and therefore the relevance of a disturbance are still recognized in several examples [24].

Furthermore, it should be pointed out that it is not necessary to bridge the several parts of the high-conducting plates at the surface. If required, the bridges could be placed further away without destroying the effect.

1	2	3
4	5	6
7	8	9

1	2	3	4
5	6	7	8
9	10	11	12
13	14	15	16

Figure 4. The segment index for $N = 2$ (left) and $N = 3$ (right).

5. CONCLUSION

We have shown that from surface currents generated in a well-defined manner the state of each MEA in a fuel cell stack can be reconstructed by tomographic methods in many cases. The following list gives examples of defects occurring in fuel cell stacks. The detectability by our scheme is based solely on the change in the current density distribution induced by the defect:

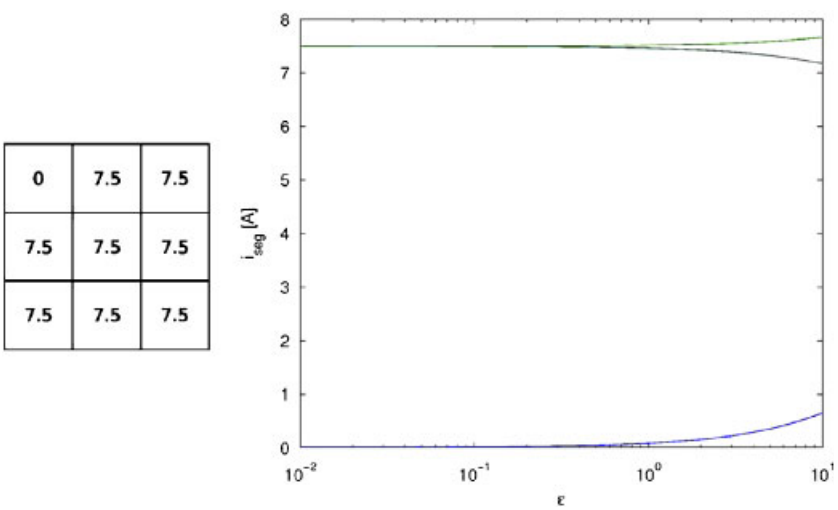

Figure 5. The lower (blue) curve represents the current across the defective segment $n = 1$. The upper decreasing (black) curve represents $n = 5, 6, 8, 9$ and the upper increasing (green) one represents $n = 2, 3, 4, 7$, respectively.

DOI: 10.1002/er

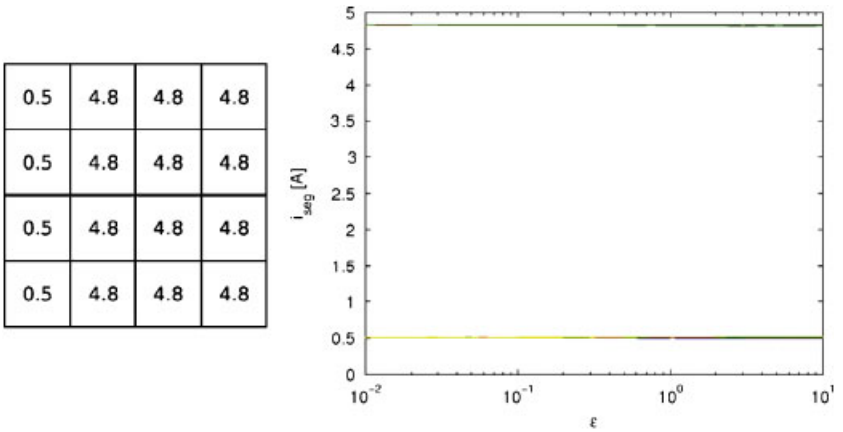

Figure 6. The lower curve represents the defective segments and the upper one the undamaged segments.

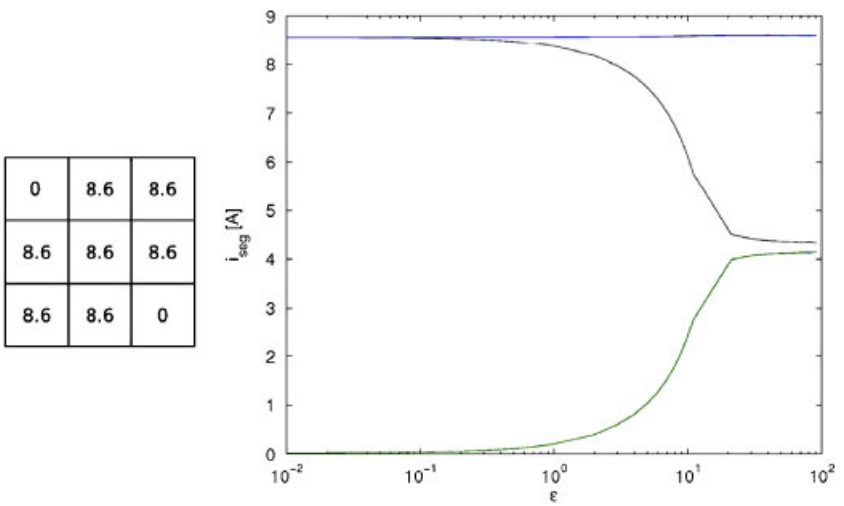

Figure 7. The lower (green) curve includes both $n = 1$ and $n = 9$, the (black) curve decreasing to $i_{seg} \approx 4\,A$ includes both $n = 3$ and $n = 7$. All other segment currents are represented by the constant curve.

- *Flooding of cathode flow fields*: If water is deposited in the cathode flow field, it blocks channels completely. Usually the channels are parallel to one slit direction, therefore the defect is limited to one stripe and can be reconstructed uniquely.
- *Flooding of the diffusion layer*: This flooding effect is not bound to a flow field channel, but as long as it is connected, its location and its severity can be detected.
- *Oxidizing of the catalyst and destruction of the membrane*: Both effects may appear at different locations of the MEA and are thus not necessarily connected. But as long as they do not emerge exactly at the same time, it is possible to detect them independently.

Even though only part of the information is obtained by measuring the surface currents, it is possible to reconstruct typical fuel cell defects. Hence the missing information is not essential and that the presented diagnostic scheme can be applied to determine the state of any MEA in a fuel cell stack.

DOI: 10.1002/er

Using our scheme change in the current distribution of each MEA in a stack can be detected. Moreover, since defects in a fuel cell lead to typical changes in the current density distribution throughout the MEA (e.g. Figure 5 shows the structure of a flooding in a flow field), it should be possible to identify defects by the structure of the current distribution.

In our calculations we have included only simple constraints. Of course, it is possible to include other constraints and further measurement data. An example is the usage of the change in the cell voltage. As extended degradations typically lead to a larger change in the cell voltage than localized ones, it is possible to determine how well a defect is localized. Another example is computing the maximal possible damage to a specific segment. If those calculations are done for each segment once, the resulting variations of the cell voltage change $U_{\text{new}} - U_0$ can be compared. By that it is possible to identify segments that are definitely not damaged [24].

We want to give a concluding comment regarding the intrinsic current density inhomogeneity of fuel cells in a stack. The intrinsic inhomogeneities give rise to transverse currents in the slitted plates. On the one hand, the presented scheme is capable of detecting these. On the other hand, by including deviations of the slit currents in the calculation, it is possible to detect defects independent of the initial current density inhomogeneity. This also holds true for already detected defects, which do not interfere with the measurement of new ones.

APPENDIX A

In this appendix we explain how we have solved Equation (4) with the constraints Equation (2), selecting the most localized solutions. The localization is achieved by minimizing f defined in Equation (7) as far as this minimization is compatible with the previous conditions.

First we replace $i_{\text{seg},n}$ by

$$x_n = i_0 - i_{\text{seg}',n} \tag{A1}$$

Inserting this, we get instead of Equation (2)

$$x_n \geqslant 0 \tag{A2}$$

instead of Equation (4)

$$\begin{gathered} \mathscr{A} \cdot \mathbf{x} - \mathbf{i}_{\text{S}} \cdot \frac{1}{I_0} \sum_{1}^{N_{\text{seg}}} x_n = \mathbf{b}, \\ b_n = \sum_{l=1}^{N_{\text{seg}}} A_{n,l} - \frac{i_{\text{S},n}}{i_0} \end{gathered} \tag{A3}$$

and

$$f(\mathbf{x}, \varepsilon) = \sum_{1}^{N_{\text{seg}}} \ln(x_n^2 + \varepsilon), \quad \varepsilon > 0 \tag{A4}$$

Defining the matrix

$$B_{m,n} = \frac{1}{I_0} i_{\text{S},m} \tag{A5}$$

we may write instead of Equation (A3)

$$(\mathscr{A} - \mathscr{B})\mathbf{x} - \mathbf{b} = 0 \tag{A6}$$

A localized solution for $\mathbf{x}$ is found by minimizing the Lagrangian

$$L(\mathbf{x}) = f(\mathbf{x}, \varepsilon) + \lambda[(\mathscr{A} - \mathscr{B})\mathbf{x} - \mathbf{b}]^2 \tag{A7}$$

while taking notice of Equation (A2) and choosing λ such that Equation (A6) is fulfilled.

A simple minimum procedure cannot be chosen since f is invariant against permutations of its coordinates which means that f has at least $N_{\text{seg}}!$ minima. From that we conclude that the Lagrangian has about as many relative minima. For such a situation a more sophisticated procedure like the genetic formalism [26] or the simulated annealing [27] method has to be applied. In the present context we have chosen the simulated annealing method and have obtained stable results with moderate computational effort.

REFERENCES

1. Mikkola M. Experimental studies on polymer electrolyte membrane fuel cell stacks. *Master Thesis*, The Helsinki University of Technology, 2001.
2. Wang L, Husar A, Zhou T, Liu H. A parametric study of PEM fuel cell performances. *International Journal of Hydrogen Energy* 2003; **28**:1263–1272.
3. Tüber K, Pócza D, Hebling C. Visualization of water buildup in the cathode of a transparent PEM fuel cell. *Journal of Power Sources* 2003; **124**:403–414.

DOI: 10.1002/er

4. Tüber K, Zobel M, Schmidt H, Hebling C. A polymer electrolyte membrane fuel cell system for powering portable computers. *Journal of Power Sources* 2003; **122**:1–8.
5. Scott K, Taama WM, Argyropoulos P. Engineering aspects of the direct methanol fuel cell system. *Journal of Power Sources* 1999; **79**:43–59.
6. Zamel N, Li X. Non-isothermal multi-phase modeling of PEM fuel cell cathode. *International Journal of Energy Research* 2009; DOI: 10.1002/er.1572
7. Yoon YG, Lee WY, Yang TH, Park GG, Kim CS. Current distribution in a single cell of PEMFC. *Journal of Power Sources* 2003; **118**:193–199.
8. Noponen M, Mennoloa T, Mikkola M, Hottinen T, Lund P. Measurement of current distribution in a free-breathing PEMFC. *Journal of Power Sources* 2002; **106**:304–312.
9. Su A, Chiu YC, Weng FB. The impact of flow field pattern on concentration and performance in PEMFC. *International Journal of Energy Research* 2005; **29**:409–425.
10. Kulikovsky AA. Electrostatic broadening of current-free spots in a fuel cell stack: the mechnism of stack aging? *Electrochemistry Communications* 2006; **8**:1225–1228.
11. Stumper J, Campbell SA, Wilkinson DP, Johnson MC, Davis M. In-situ methods for the determination of current distributions in PEM fuel cells. *Electrochimica Acta* 1998; **43**:3773–3783.
12. Yuan X, Sun JC, Wang H, Zhang J. AC impedance diagnosis of a 500 W PEM fuel cell stack Part II: individual cell impedance. *Journal of Power Sources* 2006; **161**(2):929–937.
13. Gomadam PM, Weidnern JW. Analysis of electrochemical impedance spectroscopy in proton exchange membrane fuel cells. *International Journal of Energy Research* 2005; **29**:1133–1151.
14. Mennola T, Mikkola M, Noponen M, Hottinen T, Lund P. Measurement of ohmic voltage losses in individual cells of a PEMFC stack. *Journal of Power Sources* 2002; **112**:261–272.
15. Lustfeld H, Reißel M, Schmidt U, Steffen B. Reconstruction of electric currents on a fuel cell by magnetic field measurements. *Journal of Fuel Cell Science and Technology* 2009; **6**:021012.
16. Hauer KH, Potthast R. Magnetic tomography for fuel cells—current status and problems. *Journal of Physics*: *Conference Series* 2007; **73**(1):012008.
17. Hirschfeld JA, Lustfeld H, Reißel M, Steffen B. A novel scheme for precise diagnostics and effective stabilization of currents in a fuel cell stack. *International Journal of Energy Research* 2009; submitted.
18. Lustfeld H, Reißel M, Steffen B. *Defektkontrolle für ein oder mehrere elektrische Betriebselemente*. German patent application DE: 102007061642.4-35 (20.12.2007)
19. Kim GS, St-Pierre J, Promislow K, Wetton B. Electrical coupling in proton exchange membrane fuel cell stacks. *Journal of Power Sources* 2005; **152**:210–217.
20. Kulikovsky AA. Mirroring of current-free spots in a fuel cell stack. *Journal of the Electrochemical Society* 2008; **154**:B817–B822.
21. Santis M, Freunberger SA, Papra M, Wokaun A, Büchi FN. Experimental investigation of coupling phenomena in polymer electrolyte fuel cell stacks. *Journal of Power Sources* 2006; **161**:1076–1083.
22. Freunberger SA, Schneider IA, Sui PC, Wokaun A, Djialali N, Büchi FN. Cell interaction phenomena in plymer electrolyt fuel cell stacks. *Journal of the Electrochemical Society* 2008; **155**:B704–B714.
23. Lustfeld H, Reißel M, Steffen B. Magnetotomography and electric currents in a fuel cell. *Fuel Cells—from Fundamentals to Systems* 2009; **9**:474.
24. Hirschfeld J. Tomographic problems in the diagnostics of fuel cell stacks. *Diploma Thesis*, Jül-Report Jül-4291 Forschungszentrum Jülich: Jülich, 2009. http://hdl.handle.net/2128/3588.
25. Woodbury A, Sudicky E, Ulrych TJ, Ludwig R. Three-dimensional plume source reconstruction using minimum relative entropy inversion. *Journal of Contaminant Hydrology* 1998; **32**:131–158.
26. Whitley D. A Genetic Algorithm Tutorial. *Statistics and Computing* 1994; **4**:65–85.
27. Press WH, Teukolsky SA, Vetterling WT, Flannery BP. *Numerical Recipies*. Cambridge University Press: Cambridge, 2007.